applied sciences

MDPI

Article

Research on the Improvement of Safety Navigation Based on the Shipmaster's Control of Ship Navigational Parameters When Sailing in Different Sea State Conditions

José A. Orosa [1,*], José M. Pérez-Canosa [1], Francisco J. Pérez-Castelo [2] and Vanesa Durán-Grados [3]

[1] Department of Navigation Science and Marine Engineering, University of A Coruña, Paseo de Ronda, 51, 15011 A Coruña, Spain; jose.pcanosa@udc.es
[2] Department of Industrial Engineering, University of A Coruña, 15405 A Coruña, Spain; francisco.javier.perez.castelo@udc.es
[3] Department of Thermal Engines and Machines, University of Cádiz, 11519 Cádiz, Spain; vanesa.duran@gm.uca.es
* Correspondence: jose.antonio.orosa@udc.es; Tel.: +34-981-167-000 (ext. 4320)

Abstract: Shipmasters must make several quick decisions with respect to the ship's speed and heading when new sea conditions approach. The implications for ship stability and risky situations are known but there are no guides on how they should be addressed in this limited period of time. In the present paper, and from three points of view, the ship's rolling motion in the long-term domain is analysed. Firstly, the ship's behaviour after the influence of a single and external force was studied. Secondly, the influence of successive regular beam seas, with resistance and at zero-speed conditions, was analysed. Finally, the influence of wave direction on a ship sailing at non-zero speed was investigated. Results showed that once five minutes elapse, the rolling angle tends to be null regardless of the ship's loading condition and that after a certain period of time, a coupling of the ship's rolling frequency with the waves' period and angle amplitude occurs. This circumstance was noted after three minutes for all of the ship loading conditions. Finally, novel guides for shipmasters in the form of 3D maps and polar diagrams were proposed to improve the ship's behaviour-altering navigational parameters (heading and ship's speed) when sailing in changing weather conditions. Therefore, for the three approaches, the relevant results and novel mathematical relations of linear factors were obtained which can be considered useful and applicable by the ship operators of most fishing and merchant fleets (regardless of their sizes) when they are operating under normal loading conditions.

Keywords: shipmaster's guide; ship's behaviour; rolling motion; coupling; different sea conditions; safe navigation

Citation: Orosa, J.A.; Pérez-Canosa, J.M.; Pérez-Castelo, F.J.; Durán-Grados, V. Research on the Improvement of Safety Navigation Based on the Shipmaster's Control of Ship Navigational Parameters When Sailing in Different Sea State Conditions. *Appl. Sci.* **2023**, *13*, 4486. https://doi.org/10.3390/app13074486

Academic Editor: Wenming Yang

Received: 10 March 2023
Revised: 26 March 2023
Accepted: 30 March 2023
Published: 1 April 2023

1. Introduction

The International Maritime Organization (IMO) proposed the Second Generation of Intact Stability criteria in 2020 [1]. There, five dynamic stability failure modes of sailing in waves were considered, such as parametric roll, pure loss of stability, surf-riding and broaching, dead-ship condition, and excessive accelerations [2,3]. Although all of them are a potential danger to the ship, not all of them were equally investigated. For instance, the last failure mode considered by IMO as a problem (excessive accelerations) has not been sufficiently investigated by researchers (unlike parametric roll, for instance). Parametric rolls are the most studied due to the severity of their occurrence and economic consequence, especially with registered onboard container vessels and ro-ro ships [4,5]. However, all ships are subjected to the rolling motion, considered by the literature as the most critical of the six degrees of freedom [6–8]. Furthermore, considering the periodicity of this motion, which can be established between 8 s and 18 s, during a sea journey of 24 h, a ship can roll more than 4000 full cycles, causing fatigue in the crewmembers, passengers,

instruments, equipment, and cargo lashing system. This fatigue can trigger the failure of the lashing system and put the ship's safety at risk, with negative consequences on the vessel, crewmembers, and cargo claims. In fact, many interesting research works are focused on the problems caused by the ship's rolling motion in certain equipment installed on board [9]. However, many authors agree that the study of the rolling motion is a difficult task due to the complexity of the involved problems. Some of them are the presence of external forces, which affect the ship's stability and cause great difficulty in the mathematical model proposed [10]. For that reason, traditionally mixed techniques using empirical formulas together with the most advanced experimental processes and Computational Fluid Dynamics (CFD) techniques have been used, both in damaged and intact ship conditions [6,11,12]. To conclude, the rolling angles with large amplitudes and excessive accelerations experienced by ships should be a cause of concern with respect to ensuring the safety of sea transportation.

Moreover, excessive rolling and losses of stability are one of the most important causes of capsizing [13–15]. For that reason, researchers such as Buca et al. [16] carried out interesting studies of this motion in beam waves. With a combination of parameters such as rolling angles, wave height, ship speed, and draught, they established the cause of a ship's capsizing. In addition, their research focused on capsizing, providing a ship survivability probabilistic diagram. However, in our opinion, it is not necessary to reach a capsizing condition in order to have a non-safety situation on board. Other authors [17] also worked on roll motion modelling, generating correlated stochastic processes and simulating the ship capsizing as a function of the intensity of the wave force. They concluded that under weak wave conditions, the ship finds a stationary state after a long period of time and without reaching a capsizing condition. Capsizing occurs when the ship is sailing in strong wave conditions. However, we consider that ship capsizing does not always occur in bad sea conditions. For that reason, it would desirable that the ship operator knew the elapsed period of time in which the ship begins to roll with both a constant roll angle and angular velocity (same frequency). These issues are studied in the present paper.

Regarding the periods of time in the rolling motion, relevant research works were carried out in a short-time domain [8] and using CFD [15,18]. Liu et al. [15] studied extreme roll and capsizing, which is coupled with a rapid increase in yaw angle. Sun et al. [9] also concluded that the rolling angle due to restoring momentum gradually decreases over time. However, in that paper, the range of time that could be considered depreciable could not be obtained. Furthermore, the IMO's most important regulation for calculating the minimum necessary forces to be counteracted by the lashing system of non-standardized cargo is the Cargo Stowage and Securing Code [19]. This tool considers accelerations as the main parameters to be taken into account, which in turn depend on the ship's loading condition. These transverse accelerations depend on angular velocities and therefore, on the maximum rolling angles. Although the literature [20] assumes that, at the initial state of ship design, an accurate evaluation of the ship's performance in real sea conditions becomes more imperative, in our opinion, it also becomes essential for ship operators to know the overall ship's behaviour during this motion and under the influence of beam waves. In fact, as Fan et al. [21] concluded in their study, during the ship's rolling motion, an understanding of the ship's natural period (i.e., the loading condition) is essential in order to avoid the effect of tank sloshing under different wavelengths, and vice versa, unlike the case of pitching motion.

In our opinion, it is essential for ship operators to know, on the one hand, the average time needed to reach critical rolling angle amplitudes and, on the other hand, the moment when the frequency of rolling motion is constant. The lack of knowledge of both parameters can compromise the ship's safety, triggering cargo shifting, damage to crewmembers and passengers, and even damage to the ship, in case of severe rolling.

For this reason, in the present paper, new mathematical models of the ship's behaviour in a long-time domain under the influence of a full spectrum of registered waves are proposed.

A similar approach was carried out by other authors [22], although they focused only on damaged ships during a short-time domain. Furthermore, as the tank test involves high economic costs and long preparation periods, at present, the prediction of a ship's behaviour using mathematical models is more and more commonly applied [23]. Moreover, as the weather conditions faced during sea passage may vary, the shipmaster has to make multiple decisions in order to improve the safety of navigation. Therefore, in the present research, a guide on the navigational parameters to be modified (heading and ship's speed) is proposed.

The new and original mathematical relations proposed in the present paper are applicable to the ship's behaviour during rolling both from a dynamic and static point of view in order to be as useful as possible to ship operators. This is in opposition to the traditional approach [24] where two approaches were used, i.e., from initial stability (static for $\theta < 10^{\circ}$) and dynamic stability ($\theta > 10^{\circ}$).

The present research, in the first two approaches, refers to regular beam waves, at zero-speed conditions, and uncoupled from other motions. These are considered the most unfavourable conditions when the ship is stopped. In fact, considering certain initial assumptions, the procedure was followed by many relevant and similar research works which were very similar to that proposed in the present work [7,20,23,25,26]. In a sense, the present research can be considered a continuation of previous works carried out by the authors of [27,28]. In the first of them, the rolling motion of the ship in static conditions and sailing in beam seas without a resistant environment was studied. In the second one, similar research but in dynamic conditions was carried out, where the ship's navigational parameters (heading and speed) and loading conditions, which can be modified to waves coming from any direction, were analysed.

In the present work, new mathematical models are developed. First of all, the ship's response when hit by a single external force is studied from a new point of view. In the present case, this single force is a certain wave that ceases instantly. Secondly, as this assumption is far from reality, the relationship between the different parameters of waves' full spectrum that a ship can face during sea passage is analysed. These two approaches, which correspond to the real ship's behaviour during the rolling motion in beam seas with resistance, are studied too.

Finally, after studying the influence of waves coming from any direction, with the ship at non-zero speed, a useful guide for shipmasters based on the change of heading and ship's speed was provided to be useful when experiencing changing sea conditions in order to improve safety during navigation.

Regarding the ship's characteristics which apply to the proposed models, the present research analyses the ship's loading conditions, expressed as metacentric height (GM), which in turn depends on the ship's hydrostatic values. However, as hydrostatic curves or tables would be very specific for each ship, here, the ship's natural rolling period (Td), a parameter very easy to obtain by any seafarer on board any ship, is analysed. Furthermore, it is known that, through different empirical formulas, there is a direct relationship between GM, Td, and the ship's beam. However, in order to make the present research applicable to both small fishing vessels and large merchant ships, the Td conditions of 8 s, 10 s, 12 s, and 14 s were studied. These values can be considered sufficiently representative of the majority of fishing and merchant fleets (regardless of their length) when they are operating under normal loading conditions. As the maximum initial rolling angle, 8° was selected as it is considered representative enough of an unfavourable initial situation. Concerning the sea state conditions, the full spectrum of all registered waves, with amplitudes from 0.08 to 22.92 m, and an average rolling damping factor of 0.015 was selected for modelling according to the literature.

2. Materials and Methods

2.1. Ship's Rolling Motion in Calm Waters in a Resistant Environment

This sub-section provides a study of the ship's behaviour affected by an external single force which, once transversally applied, disappears. In zero-speed conditions, when studying the ship's rolling motion in calm waters and without resistance, the equality between the moments intervening in the ship and the inertia moments is expressed as follows:

$$Ig \cdot \frac{d^2\theta}{dt^2} + Ma = 0 \quad (1)$$

where, in accordance with the Table A1, Ma is the ship's righting moment and Ig is the inertia moment of the ship's mass along the longitudinal axis passing through its centre of gravity. In this stage, as it is not considered a resistant environment, the involved moments are only the righting moments.

However, in the equation of the rolling motion in calm waters with resistance, three forces are considered: the inertia forces, the forces of water and air, and the ship's righting moment. In the present case, the rolling motions considered are isochronous and the amplitude of the rolling angles decreases due to the resistances of water and air. On the one hand, in order to define the resistance moment, it is established that the resistance is proportional to the rolling angle amplitude. On the other hand, the amplitude of successive rolling angles decreases and then the resistance also decreases, while other parameters such as the ship's displacement and metacentric height (GM) are constant values for a certain ship's loading condition. Due to isochronism, the angular velocity also decreases, and, in consequence, it can be concluded that the resistant moment is linearly proportional to the angular velocity of the ship's rolling motion. This approximation is valid enough to establish the relationship between the ship's natural rolling period (Td) with and without resistance. Therefore, in the new proposed model in the present paper, the application of linear factors is assumed.

In the equation for the rolling motion (Equation (2)) in a resistant environment in calm waters, the inertia forces (first term), the forces of water and air (second term), and the ship's righting moment (third term) interact as follows:

$$Ig \cdot \frac{d^2\theta}{dt^2} + A_R \frac{d\theta}{dt} + D \cdot GM \cdot \theta = 0, \quad (2)$$

where A_R is the damping coefficient and D is the ship's displacement.

In order to obtain the equation for the rolling motion with resistance as a function of the ship's loading condition, several transformations were performed on Equation (2). Dividing this equation by Ig, we obtain:

$$\frac{d^2\theta}{dt^2} + \frac{A_R}{Ig} \frac{d\theta}{dt} + \frac{D \cdot GM}{Ig} \cdot \theta = 0, \quad (3)$$

with inertia being:

$$I_g = \frac{D}{g} \cdot k^2, \quad (4)$$

where K is the turning radius of the ship's mass. Solving for operational convenience:

$$2\lambda = \frac{A_R}{I_g} = \frac{A_R \cdot g}{D \cdot k^2}, \quad (5)$$

and replacing Equation (5) in Equation (3), we find:

$$\frac{d^2\theta}{dt^2} + 2\lambda \frac{d\theta}{dt} + \frac{D \cdot GM}{\frac{D}{g} \cdot k^2} \cdot \theta = 0, \quad (6)$$

$$\frac{d^2\theta}{dt^2} + 2\lambda \frac{d\theta}{dt} + \frac{g \cdot GM}{k^2} \cdot \theta = 0. \quad (7)$$

Furthermore, knowing that:

$$\omega^2 = \frac{g \cdot GM}{k^2}, \quad (8)$$

and introducing Equation (8) in Equation (7), the following is expressed:

$$\frac{d^2\theta}{dt^2} + 2\lambda \frac{d\theta}{dt} + \omega^2 \cdot \theta = 0, \quad (9)$$

where Equation (9) is the differential equation of the rolling motion in calm waters with resistance. According to other studies of damped oscillatory motions, the necessary auxiliary equation for the analysis and development of this equation is:

$$m^2 + 2\lambda \cdot m + \omega^2 = 0, \quad (10)$$

The solutions to which are:

$$m = \frac{-2\lambda \pm \sqrt{(2\lambda)^2 - 4\omega^2}}{2}, \quad (11)$$

$$m_1 = -\lambda + \sqrt{\lambda^2 - \omega^2}, \quad (12)$$

$$m_2 = -\lambda - \sqrt{\lambda^2 - \omega^2}. \quad (13)$$

The difference $(\lambda^2 - \omega^2)$ gives rise to three different cases with different solutions. It is, therefore, necessary to analyse the three possibilities and, afterwards, develop the case corresponding to the rolling motion.

In the first case, when $(\lambda^2 - \omega^2) > 0$, the damping factor ($A_R$) is high, and an overdamped system is produced. In this case, the solution for Equation (9) represents a smooth and non-oscillating rolling motion.

In the second case, when $(\lambda^2 - \omega^2) = 0$, its equation represents a non-oscillating motion. However, any decrease in the damping force (λ) converts to $(\lambda^2 - \omega^2)$ in a value negative, which would be the third case. These conditions are called critically damped. Therefore, when $(\lambda^2 - \omega^2) < 0$, the roots of Equations (12) and (13) are negatives and, in consequence, they give rise to complex numbers:

$$m_1 = -\lambda + \sqrt{\omega^2 - \lambda^2} \cdot i\,, \quad (14)$$

$$m_1 = -\lambda - \sqrt{\omega^2 - \lambda^2} \cdot i\,. \quad (15)$$

Consequently, Equation (9) can be expressed as follows:

$$\theta = e^{-\lambda \cdot t} \left[c_1 \cdot \cos \sqrt{\omega^2 - \lambda^2} \cdot t + c_2 \cdot \sin \sqrt{\omega^2 - \lambda^2} \cdot t \right], \quad (16)$$

where Equation (16) describes the ship's own oscillatory motion, called underdamped. Therefore, this is the most interesting case for the present research.

If some terms in Equation (16) are replaced by Equation (17):

$$\omega_1^2 = \omega^2 - \lambda^2, \quad (17)$$

$$\theta = e^{-\lambda \cdot t} [c_1 \cdot \cos \omega_1 \cdot t + c_2 \cdot \sin \omega_1 \cdot t] , \quad (18)$$

where ω_1 is the damped ship's natural roll frequency.

Considering that when t = 0, the rolling angle (θ) reaches the maximum value (θ_M), and then the angular velocity $d\theta/dt$ is zero. In Equation (18), for t = 0 and $\theta = \theta_M$:

$$e^{-\lambda \cdot t} = 1, \quad (19)$$

$$c_1 \cdot \cos \omega_1 \cdot t = c_1, \quad (20)$$

$$c_2 \cdot \sin \omega_1 \cdot t = 0, \quad (21)$$

Therefore, $c_1 = \theta_M$. Deriving Equation (18) according to the chain rule:

$$\frac{d\theta}{dt} = -\lambda \cdot e^{-\lambda \cdot t} [c_1 \cdot \cos \omega_1 \cdot t + c_2 \cdot \sin \omega_1 \cdot t] + e^{-\lambda \cdot t} [-c_1 \cdot \omega_1 \cdot \sin \omega_1 \cdot t + c_2 \cdot \omega_1 \cdot \cos \omega_1 \cdot t], \quad (22)$$

with the angular velocity equal to zero leads to:

$$0 = -\lambda \cdot e^{-\lambda \cdot t} [c_1 \cdot \cos \omega_1 \cdot t + c_2 \cdot \sin \omega_1 \cdot t] + e^{-\lambda \cdot t} [-c_1 \cdot \omega_1 \cdot \sin \omega_1 \cdot t + c_2 \cdot \omega_1 \cdot \cos \omega_1 \cdot t], \quad (23)$$

removing terms results in:

$$0 = -\lambda \cdot c_1 + c_2 \cdot \omega_1, \quad (24)$$

and knowing that $c_1 = \theta_M$ we can find:

$$0 = -\lambda \cdot \theta_M + c_2 \cdot \omega_1. \quad (25)$$

Clarifying the c_2 value in Equation (25):

$$c_2 = \frac{\lambda \cdot \theta_M}{\omega_1} , \quad (26)$$

and replacing c_1 and c_2 in Equation (18), it is observed:

$$\theta = e^{-\lambda \cdot t} \left[\theta_M \cdot \cos \omega_1 \cdot t + \frac{\lambda \cdot \theta_M}{\omega_1} \cdot \sin \omega_1 \cdot t\right] , \quad (27)$$

$$\theta = \theta_M \cdot e^{-\lambda \cdot t} \left[\cos \omega_1 \cdot t + \frac{\lambda}{\omega_1} \cdot \sin \omega_1 \cdot t\right] . \quad (28)$$

Consequently, Equation (28) represents the ship's rolling motion in calm waters and with resistance after the influence of a single and external force transversally applied.

2.2. Waves Spectrum

The full spectrum of regular and trochoidal waves was already studied by authors in previous research works [27,28] where the influence of the waves' full spectrum on the ship's behaviour was analysed. The present paper is not intended to study the influence of the waves' full spectrum on the ship's rolling motion. However, it is necessary to establish the characteristics of the mathematical models used for the studied cases of certain waves. For practical purposes, and according to other relevant research works, the waves are considered regular, where the analysed parameters are the following: wave period (Tw), translation velocity (Vw), and wavelength (Lw).

With the help of empirical observations [29] and considering these three parameters, 21 sea state conditions were registered; their characteristics are shown in Table 1. The following polynomial regression equations were obtained:

$$\mathrm{Lw\ (m)} = 1.5838 \cdot \mathrm{Tw}^2 - 0.5558 \cdot \mathrm{Tw} + 1.4737, \quad (29)$$

$$\mathrm{Vw\ (knots)} = -0.0006 \cdot \mathrm{Tw}^2 + 1.5196 \cdot \mathrm{Tw} + 0.1165, \quad (30)$$

$$\mathrm{Vw\ (m \cdot s^{-1})} = 0.0009 \cdot \mathrm{Tw}^2 + 0.7632 \cdot \mathrm{Tw} + 0.3669, \quad (31)$$

Table 1. Parameters of regular waves' full spectrum.

Tw (s)	Lw (m)	Vw (m·s^{-1})	Vw (Knots)	Hw (m)	Aw (m)
1	2.5017	1.131	1.6355	0.08	0.04
2	6.6973	1.8969	3.1533	0.22	0.11
3	14.0605	2.6646	4.6699	0.47	0.23
4	24.5913	3.4341	6.1853	0.82	0.41
5	38.2897	4.2054	7.6995	1.28	0.64
6	55.1557	4.9785	9.2125	1.84	0.92
7	75.1893	5.7534	10.7243	2.50	1.25
8	98.3905	6.5301	12.2349	3.28	1.64
9	124.7593	7.3086	13.7443	4.15	2.08
10	154.2957	8.0889	15.2525	5.14	2.57
11	186.9997	8.871	16.7595	6.23	3.11
12	222.8713	9.6549	18.2653	7.42	3.71
13	261.9105	10.4406	19.7699	8.72	4.36
14	304.1173	11.2281	21.2733	10.13	5.06
15	349.4917	12.0174	22.7755	11.64	5.82
16	398.0337	12.8085	24.2765	13.25	6.63
17	449.7433	13.6014	25.7763	14.98	7.49
18	504.6205	14.3961	27.2749	16.80	8.40
19	562.6653	15.1926	28.7723	18.74	9.37
20	623.8777	15.9909	30.2685	20.78	10.39
21	688.2577	16.791	31.7635	22.92	11.46

The graphs shown in Figure 1 corresponding to Equations (29)–(31) reveal a very high precision for the determining factor.

Furthermore, according to Equation (10), it is established that there is a direct relationship between the wave height (Hw), the wavelength (Lw), and the sinus of wave maximum slope (θ_{MW}). Moreover, this θ_{MW} is constant and equal to 0.1047 rad (6°), regardless of sea state condition.

$$\sin(\theta_{MW}) = \pi \cdot \frac{\mathrm{Hw}}{\mathrm{Lw}}, \quad (32)$$

Using Equation (32) and the wavelength calculated as per Equation (29), Hw and wave amplitude (Aw), i.e., half of Hw, are obtained. Therefore, the full spectrum of the regular waves studied in the present work is based on the results included in Table 1.

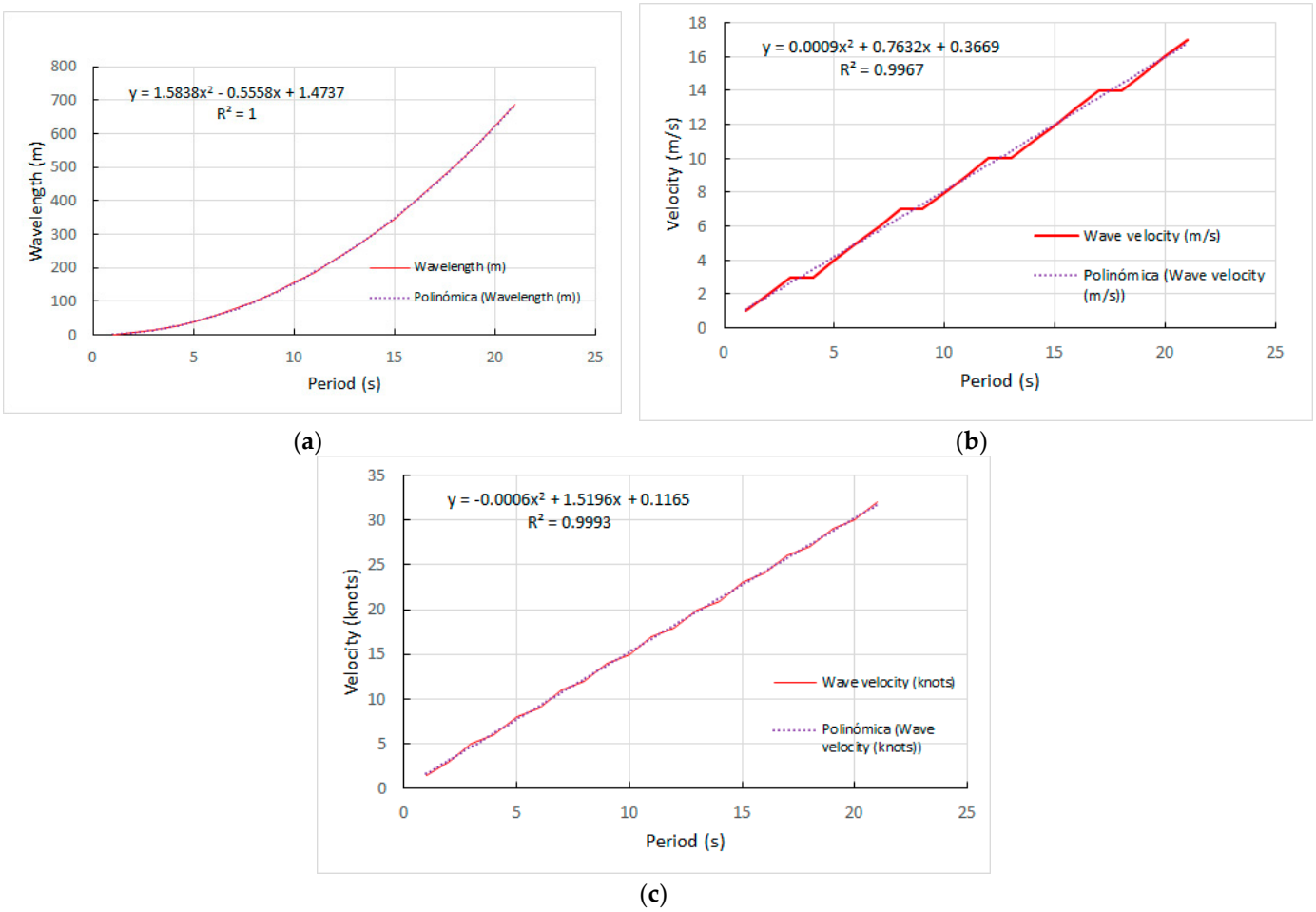

Figure 1. (**a**) Wavelength as a function of period. Precision 100%. (**b**) Velocity in $m \cdot s^{-1}$ as a function of period. Precision 99.67%. (**c**) Velocity in knots as a function of period. Precision 99.93%.

2.3. Ship's Rolling Motion Affected by Successive Beam Waves in a Resistant Environment

The hypothesis referred to in Section 2.1 can only be considered theoretical, because, in real conditions, ships are not only under the influence of a single wave (single force) but are subject to the influence of successive waves. For this reason, the effect of beam seas on an idle ship, together with the ship's behaviour as a consequence of its righting moment, is studied in the present sub-section.

The rolling response of a ship under the influence of any beam wave is called its induced rolling motion (θf). This induced force is determined by the parameters of waves (maximum wave slope, θ_{MW}, and frequency, ω_W), and by the ship parameters (the ship's natural rolling period, Td). This induced force can be expressed as follows [28]:

$$\theta f = \frac{\theta_{MW} \cdot \cos\beta \cdot \sin[\omega_W \cdot t - \beta]}{1 - \frac{Td^2}{Tw^2}} = \frac{\theta_{MW} \cdot \cos\beta \cdot \sin\left[\frac{2\pi}{Tw} \cdot t - \beta\right]}{1 - \frac{Td^2}{Tw^2}}, \quad (33)$$

where β is equal to:

$$\tan\beta = \frac{\lambda_1}{\pi} \cdot \frac{\frac{Td}{Tw}}{1 - \frac{Td^2}{Tw^2}}, \quad (34)$$

Therefore, taking into account Equation (28) and the induced rolling by successive waves, the equation of the rolling angle in zero-speed conditions and under the influence of beam waves is the following:

$$\theta = \theta_M \cdot e^{-\lambda \cdot t} \cdot \left[\cos(\omega_1 \cdot t) + \frac{\lambda}{\omega_1} \cdot \sin(\omega_1 \cdot t)\right] + \frac{\theta_{MW} \cdot \cos\beta \cdot \sin(\omega_W \cdot t - \beta)}{1 - \frac{Td^2}{Tw^2}}, \quad (35)$$

or

$$\theta = \theta_M \cdot e^{-\lambda \cdot t} \cdot \left[\cos\sqrt{\omega^2 - \lambda^2} \cdot t + \frac{\lambda}{\sqrt{\omega^2 - \lambda^2}} \cdot \sin\sqrt{\omega^2 - \lambda^2} \cdot t\right] + \frac{\theta_{MW} \cdot \cos\beta \cdot \sin(\omega_W \cdot t - \beta)}{1 - \frac{Td^2}{Tw^2}}, \quad (36)$$

For operative purposes, replacing the ship's natural frequency, ω, with its relationship with Td, we obtain the following:

$$\theta = \theta_M \cdot e^{-\lambda \cdot t} \cdot \left[\cos\sqrt{\left(\frac{2\pi}{Td}\right)^2 - \lambda^2} \cdot t + \frac{\lambda}{\sqrt{\left(\frac{2\pi}{Td}\right)^2 - \lambda^2}} \cdot \sin\sqrt{\left(\frac{2\pi}{Td}\right)^2 - \lambda^2} \cdot t\right] + \frac{\theta_{MW} \cdot \cos\beta \cdot \sin(\omega_W \cdot t - \beta)}{1 - \frac{Td^2}{Tw^2}}. \quad (37)$$

2.4. Ship's Rolling Motion at Non-Zero Speed and under the Influence of Waves Coming from Any Constant Direction

As the hypotheses referred to previously are not universal, in the present sub-section the ship's rolling motion when the ship is sailing with zero speed is studied. In this real situation, the ship is receiving the impact of successive waves from a constant direction, α, defined as the angle formed between the ship's centre line (heading) and the waves' direction. Navigational parameters such as the ship's speed (Vs) and heading are under the control of the ship's operator (the decision criteria of the shipmaster), and both parameters are present as the only tools which can modify the ship's behaviour under certain weather conditions, given that they cannot be controlled by sailors. In this dynamic situation, the encounter velocity (Ve) is defined as follows [28]:

$$Ve = Vw + Vs \cdot \cos\alpha \quad (38)$$

where Vw is the wave's velocity.

Sailing in these dynamic conditions, the parameter to be monitored by the duty officer on board to control the ship's navigation safety is the encounter period (Te), instead of Tw. This Te can be expressed as follows:

$$Te = \frac{Lw}{Vw + Vs \cdot \cos\alpha} \quad (39)$$

or

$$Te = \frac{Tw}{1 + \frac{Vs}{Vw} \cdot \cos\alpha} \quad (40)$$

Equation (39) defines the encounter period (Te) as a function of the given wave's characteristics (Tw and Vw), and the navigational parameters (Vs and α). A shipmaster's knowledge of the Te is essential to make decisions to improve the ship's behaviour and safety. Despite this, this analysis is not performed in detail at the time these situations occur, rather, decision-making is replaced by navigation experience, and, in consequence, several accidents can occur.

According to our previous research work [28], it can be concluded that it is possible to modify the effect of sailing in different sea conditions on a ship based on the Te concept. In addition, by acting on the heading and ship's speed, it is possible to adapt to unfavourable sea conditions to have a friendlier effect on a ship. This is something commented on by sailors and defined by naval architects' designs, but no mathematical guide is employed for the optimisation of the decision-making in the reduced time of coupling.

Furthermore, it is known that, in dynamic situations, the maximum rolling angle is registered on board with the following periodicity:

$$t = \left(\frac{(2 \cdot n + 1)}{4}\right) \cdot Te + \frac{Te}{2\pi} \cdot \beta \quad (41)$$

Although it is important to note that this maximum rolling angle is relative, so it does not always have the same amplitude.

3. Results

In this section, firstly, the results of the ship's behaviour affected by a single external force to which the ship reacts as a consequence of the initial restoring moment, defined by the metacentric height (GM), are analysed. As the GM is a parameter that depends on the ship's hydrostatic values, the present study considers the Td as the value which represents the ship's loading condition. Furthermore, the Td can be easily measured by the ship operators and is a parameter applicable to any type of ship. Afterwards, the influence of certain sea state conditions on the ship's rolling motion is studied, obtaining generic conclusions valid for the full wave spectrum. It is remarkable to note that in these initial simulations, beam waves are used because they are considered the worst condition for the general ship's safety.

Regarding the ship's parameters used in the simulations, certain loading conditions (GM) were selected to be as representative as possible of all merchant fleets and even applicable to fishing vessels.

The GM has a direct relationship with the Td and the ship's beam [30]. However, the GM is a very difficult to calculate parameter because it is variable for each ship during a certain sea passage; therefore, a range of Td values, which are usually found, is used. According to several empirical calculations included in the literature [31,32], Td values of 8 s, 10 s, 12 s, and 14 s were studied [33].

The resistant environment during the rolling motion is produced mainly by the water. Air resistance can be underestimated due to its minimum effect, or directly included in the rolling damped factor, λ.

According to the literature review, a λ value of 0.015 was selected as representative of the average coefficient for the successive rolling angles with different amplitudes, where λ is changed [34].

Regarding the maximum initial rolling angle, θ_M, 8.0° was selected as representative of what is considered, in the field of ship's theory, to be the initial intact stability.

Therefore, the ship parameters and initial conditions used in the simulations of the two first sub-sections were as follows:

- Ship in the upright position;
- An average maximum initial rolling angle (θ_M) of 8°;
- Ship's loading condition (Td) at 8 s, 10 s, 12 s, and 14 s;
- Rolling damping factor (λ): of 0.015;
- Ship at zero-speed condition.

3.1. Ship's Rolling Motion in Calm Waters in a Resistant Environment

In this sub-section, the ship's behaviour with different loading conditions (Td) in a linear time domain under the influence of a single external force is presented with the ship in the idle condition.

By analysing the $e^{-\lambda \cdot t}$ factor from Equation (28), it can be predicted that when time (t) is infinite, the rolling angle amplitude tends to be zero. However, when the rolling angles are represented graphically over time, as shown in Figure 2, it is seen that in all cases of the ship's loading condition (Td = 8 s, 10 s, 12 s, and 14 s), the rolling angle tends to be null in the same time range, around 300 s. The only difference between the different studied cases is the frequency of the rolling angles approaching zero. This can be considered a very

relevant result which, to some extent, contradicts what is traditionally assumed, that is, the greater the stability (lower Td), the less time to recover the upright position and vice versa. What is more, regardless of the ship's loading conditions, the elapsed time for it to recover the upright condition is the same, in all cases.

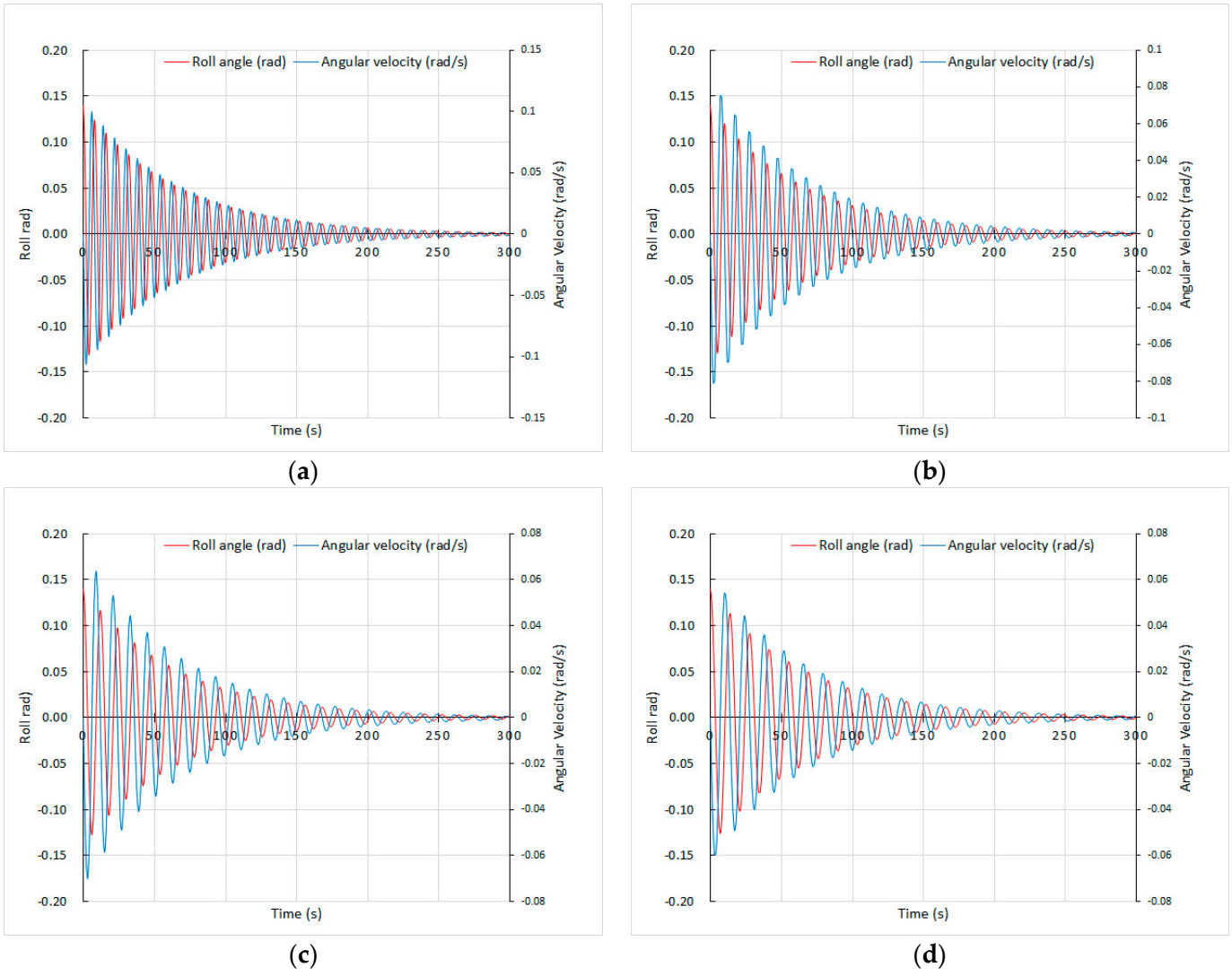

Figure 2. Rolling angle and the corresponding angular velocity for different loading conditions. (**a**) Td = 8 s, (**b**) Td = 10 s, (**c**) Td = 12 s, and (**d**) Td = 14 s.

Furthermore, as can be observed from Figure 2, in the four represented cases, after the same period of time has elapsed, the roll amplitude is practically the same. This is another important issue because the supposed advantage of greater stability (Td = 8 s, Figure 2a) does not translate into a lower rolling angle amplitude. Therefore, from this point of view, it would be better to have less stability (Td = 14 s, Figure 2d) because the comfort of crew members and/or passengers would be much better. In addition, equipment fatigue would be reduced.

In order to verify that the only difference in the ship's behaviour between the different studied cases is the frequency of rolling angles, which tend to be zero, the equation of angular velocity, corresponding to the initial restoring moment (θ'_{RM}), was obtained. The angular velocity is calculated by the following equation:

$$\theta'_{RM} = \theta_M \cdot e^{-\lambda \cdot t} \cdot [\lambda \cdot \cos(\omega_1 \cdot t) - \omega_1 \cdot \sin(\omega_1 \cdot t)] - \theta_M \cdot \lambda \cdot e^{-\lambda \cdot t} \cdot \left[\cos(\omega_1 \cdot t) + \frac{\lambda}{\omega_1} \cdot \sin(\omega_1 \cdot t)\right], \quad (42)$$

Figure 2 shows, on each of the rolling angle graphs for each loading condition, the corresponding angular velocity as per Equation (42). From them, it can be deduced that the frequency, understood as the velocity in harmonic motion, corresponds with the previously mentioned relevant results.

Once it was graphically demonstrated in Figure 2 that after the first 300 s the ship's rolling motion with any loading condition is practically nil, the exponential limit curve valid for any ship's loading condition, which represents the maximum rolling angle, was plotted as shown in Figure 3. The obtained relevant result can be expressed by the term $\theta_M \cdot e^{-\lambda \cdot t}$, and it can be applicable to any type of vessel.

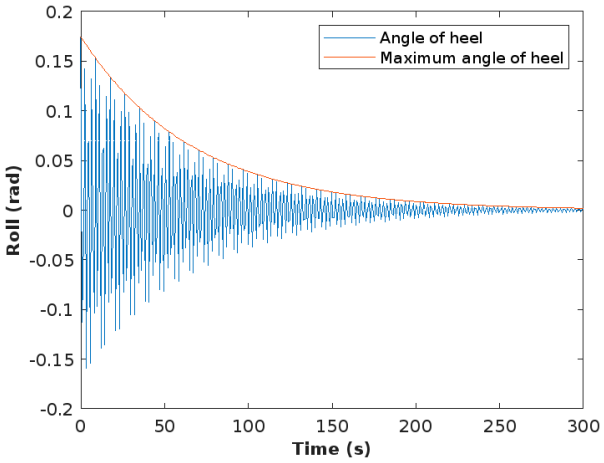

Figure 3. Representation (red colour) of the exponential limit curve of a ship's rolling motion under the influence of a single and external force.

According to this mathematical term, represented in the red colour in Figure 3, it is possible to calculate the time to reach a certain rolling angle proposed by the ship operator. Therefore, it is a useful tool available for ship operators to know, for example, the time available to change the ship's loading condition, improving the ship's behaviour.

3.2. Ship's Rolling Motion Influenced by Successive Beam Waves in a Resistance Environment

This sub-section provides the results of a realistic ship's behaviour under the influence of beam seas, which affect the ship's rolling motion successively, just as it happens in a regular swell.

As it was mentioned in Section 2.2, the real sea state conditions are referred to by 21 different types. However, the focus of this sub-section is not to analyse the influence of all the waves in the spectrum on a certain ship's loading condition, it is to obtain conclusions about the ship's performance under the influence of certain types of waves, which can be used for the rest. With this approach, as the weather conditions cannot be modified, the ship operator has an idea about the ship's final behaviour after a relatively long period of elapsed time (t).

With the objective of obtaining a similar approach to Section 2.1, Figure 4 represents Equation (37) for a Tw = 18 s, which is considered a very bad sea state condition, corresponding to a wave amplitude (Aw) of 8.40 m, i.e., a wave height of 16.80 m. As seen in Figure 4, it is remarkable to note that between 150 s and 200 s onwards, a coupling of the rolling frequencies with the Tw occurs for all of the ship loading conditions (Td) simulated, periodically repeated, and with the same rolling angle amplitudes, which depend on each ship's loading condition. What is the same, once the mentioned period of time has elapsed, the ship begins to roll according to the wave's frequency and with the same amplitude, regardless of its loading condition.

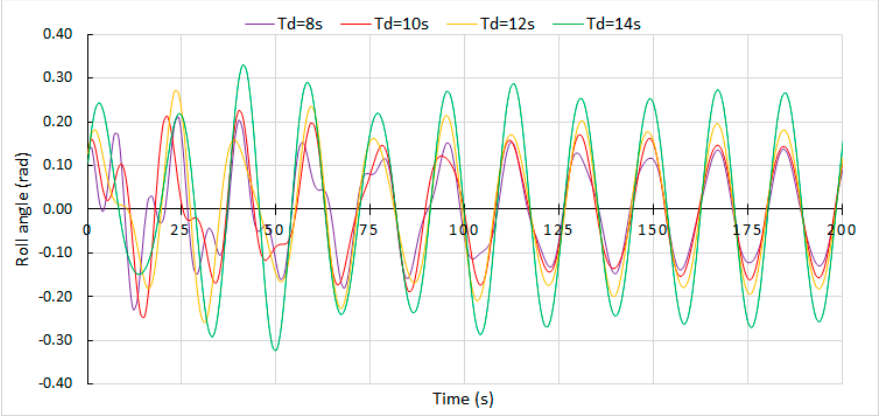

Figure 4. Rolling angles reached by different ship loading conditions for Tw = 18 s.

In order to validate these remarkable results, it was necessary to obtain the corresponding angular velocities. In this case, the angular velocity of Equation (35) in a dynamic condition of waves, θ'_W, can be expressed as follows:

$$\theta'_W = \theta_M \cdot e^{-\lambda \cdot t} \cdot [\lambda \cdot \cos(\omega_1 \cdot t) - \omega_1 \cdot \sin(\omega_1 \cdot t)] - \theta_M \cdot \lambda \cdot e^{-\lambda \cdot t} \cdot \left[\cos(\omega_1 \cdot t) + \frac{\lambda}{\omega_1} \cdot \sin(\omega_1 \cdot t)\right] - \frac{\theta_{MW} \cdot \omega_W \cdot \cos(\beta - \omega_W \cdot t) \cdot \cos\beta}{\frac{Td^2}{Tw^2} - 1}, \quad (43)$$

In Figure 5, the angular velocity for the same sea state condition (Tw = 18 s) and for the same studied cases, i.e., Td = 8 s, 10 s, 12 s, and 14 s, are plotted. These results indicate again that between 150 s and 200 s, a perfect coupling of the ship's own angular velocities is produced with the motion of the angular velocities produced by the waves.

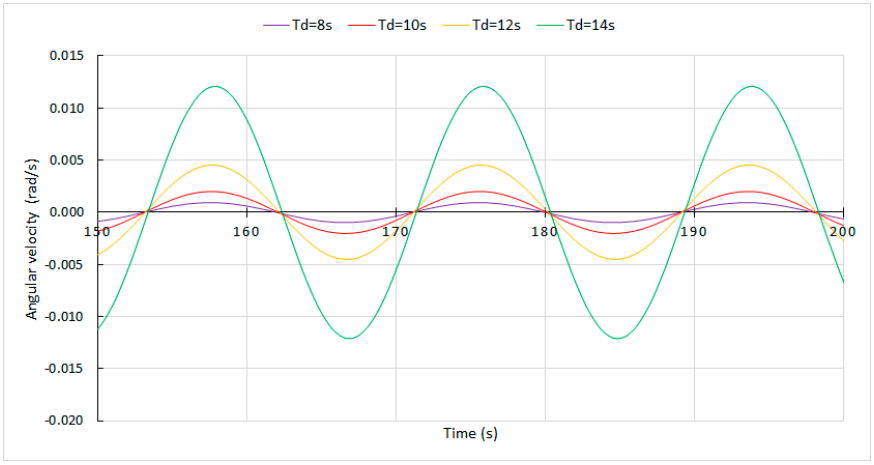

Figure 5. Rolling angular velocities reached by different ship loading conditions for Tw = 18 s.

In order to show the coupling process produced between both frequencies (the ship and waves) after the first 150–200 s under the influence of the waves, regardless of the ship's and wave parameters, the rolling angle produced by induced forces of waves with a Tw = 12 s and where the ship has a Td = 9 s (yellow colour) is shown in Figure 6. Over this graph, the exponential limit curve (purple colour) is also plotted where it is deducted that, from 150 to 200 s onwards, a perfect coupling of the ship to the waves' frequencies is registered, keeping the amplitude of the rolling angles constant over time.

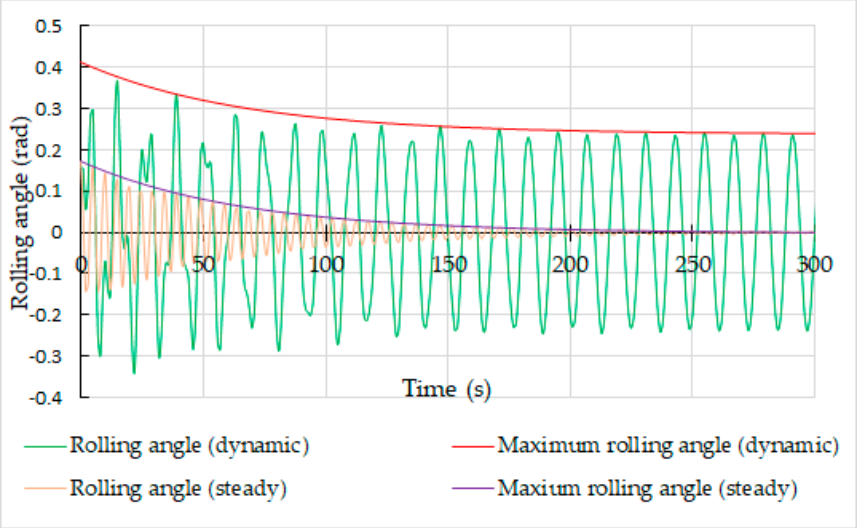

Figure 6. Representation of the maximum rolling angles in static (due to a single and external force) and in dynamic conditions (under the influence of successive waves) and their corresponding exponential limit curves.

Furthermore, and for comparative purposes, in the same Figure 6, the rolling angles originating from the intact stability (Td = 9 s) as a result of a single external force (blue colour) and the corresponding exponential limit curve (red colour) are depicted, where it is observed that, after the first 300 s, the roll angles are practically null.

It is worth noting that in order to define the time (t) in which the final coupling is reached, it is necessary to define the minimum admissible rolling angle (θ_{MIN}). For this reason, in dynamic conditions at zero speed, i.e., receiving the impact of successive waves, it was chosen as 0.23 rad. Then, for a given Td and Tw, and establishing the minimum admissible rolling angle (θ_{MIN}), it is possible to determine the time (t) of the coupling from the following equation:

$$\theta_{MIN} = \theta_M \cdot e^{-\lambda \cdot t} + \frac{\theta_{MW}}{1 - \frac{Td^2}{Tw^2}}, \quad (44)$$

As it was mentioned, in our simulations, certain sea state conditions valid for the full spectrum of waves were selected. However, in the particular cases when a Tw < Td was selected, relevant results are also obtained, which are different from the previously commented. For instance, in the studied cases of Td = 8 s, 10 s, 12 s, and 14 s, if waves of Tw = 11 s are selected, the corresponding rolling angles plotted in Figure 7 are reached.

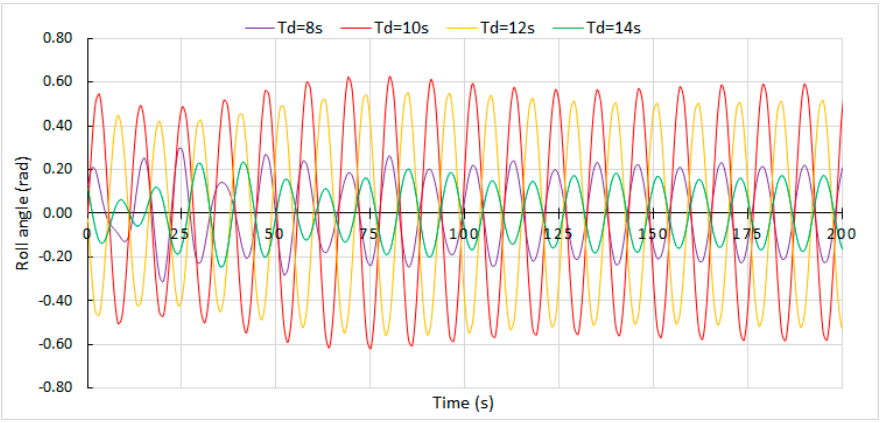

Figure 7. Rolling angles reached by different ship loading conditions for Tw = 11 s.

From Figure 7, it can be concluded that the results regarding the coupling are being produced in the same periods, i.e., after the first 150–200 s. Nevertheless, it is remarkable that for Td = 8 and 10 s, the rolling angles occur on the opposite side when Td = 12 and 14 s. Considering that the simulated waves were Tw = 11 s, it can be deduced that if Td < Tw, the rolling angles will be produced on the opposite side as that of Td > Tw. What is more, a constant lag equivalent to half of Td is registered between both situations, regardless of the Td value.

Furthermore, in order to have a more detailed idea of the ship's behaviour at the first moment after being influenced by successive waves, the case where Tw = 5 s, which corresponds to a very smooth condition, was simulated. Figure 8 shows the rolling angles in the first 100 s, where the ship's erratic behaviour between the different loading conditions is observed, unlike what is observed in Figure 9, in which with a Tw = 18, i.e., very rough sea conditions, a more harmonious and smooth ship behaviour can be seen. Despite this, as it has been concluded, in any case, a full coupling will take place, regardless of the ship's loading conditions and always at the same range of time.

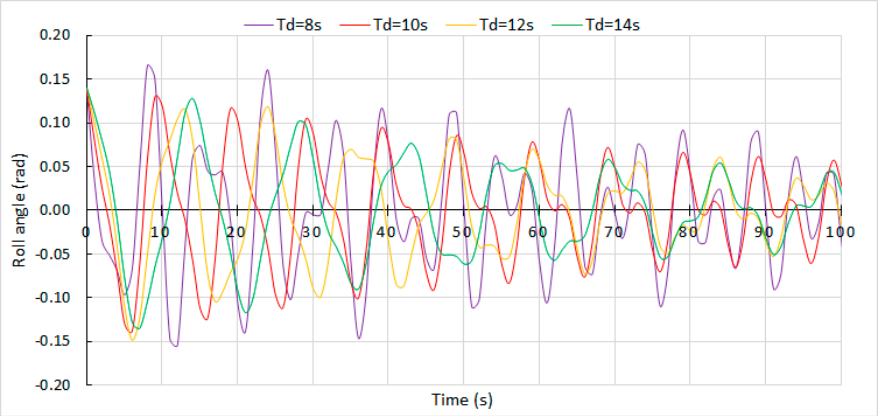

Figure 8. Simulation of the rolling angle for Tw = 5 s in the first moments.

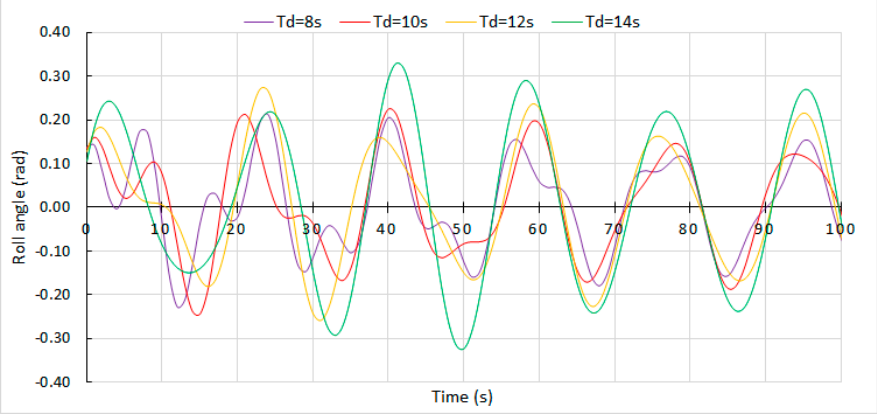

Figure 9. Simulation of the rolling angle for Tw = 18 s in the first moments.

Once it was shown that a coupling between the sea state conditions and the ship's behaviour is produced, the approximate instants when the coupling with the Tw is produced was represented in Figure 10. These moments were established when the rolling angle amplitude was almost constant. It should be noted that at the lowest values of Tw, the coupling time would tend to infinity, due to the force generated by very smooth waves, which has hardly any influence on the ship's behaviour. For this reason, the tendency of the ship will be to roll according to its restoring moment.

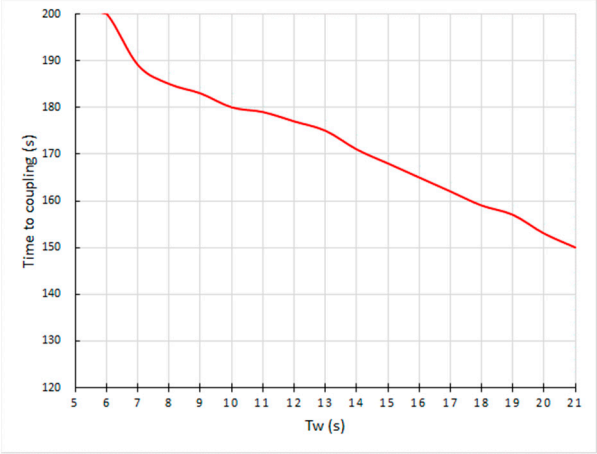

Figure 10. Time to coupling depending on the Tw state.

3.3. Ship's Rolling Motion at Non-Zero Speed and under the Influence of Waves Coming from Any Constant Direction

This sub-section shows the results which can be considered as a practical guide for shipmasters to take into account when sailing under given weather conditions.

Considering the real sea state conditions previously studied, for practical purposes, two waves of the full spectrum were selected. The first one was Tw = 6 s, considered as smooth conditions, and the second one was Tw = 18 s, which represents a rough sea state.

Regarding the ship's speed, a range from 2 to 20 knots was analysed, with intervals of 2 knots, knowing that in many ships of a merchant fleet, the minimum speed is over 5 knots. However, speeds lower than 5 knots were considered in order to be useful to small and medium fishing vessels too.

With regards to the heading angle, α, changes of 10° were considered, from 000° to 180°, as 10° is understood to be the minimum alteration to steering the ship and improve its behaviour under bad weather conditions.

Considering Equation (40), Figure 11 represents the needed Te of a ship sailing at a certain speed and for all heading alterations considered for a Tw = 18 s. As it can be observed, for heading alterations $\alpha < 90°$, i.e., receiving the seas between the forward and the beam, the Te decreases with increasing ship speed. For $\alpha = 90°$, the Te is constant, regardless of the ship's speed, and it matches exactly with Tw, due to the intervention of cos α. This particular case, and at zero-speed conditions, would correspond with those studied in the previous sub-sections, i.e., under the influence of beam seas. Furthermore, it can be concluded that for $\alpha > 90°$, Te increases as the ship's speed increases. The highest time of Te occurs for $\alpha = 180°$, i.e., sailing following seas.

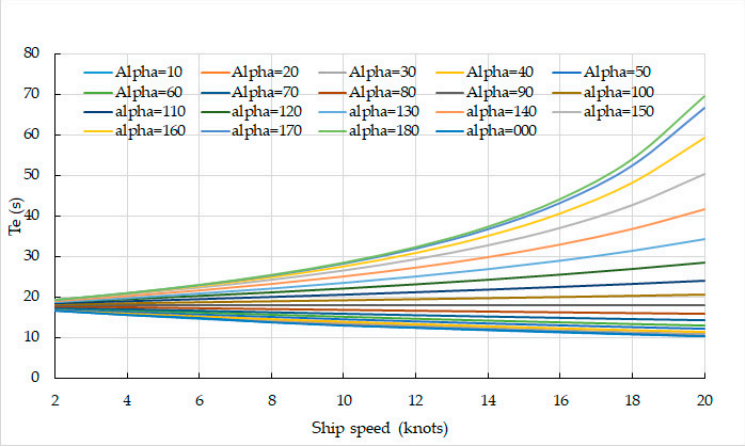

Figure 11. Te for different combinations of ship speeds and α angles, for a Tw = 18 s.

In Figure 12, the influence of Tw = 6 s in the relationship between the navigational parameters of ship speed and heading (or α angle) is depicted. For clarifying purposes, the results were plotted on two graphs, i.e., an α angle between 000° and 90° (Figure 12a), and α angle from 90° to 180° (Figure 12b). In Figure 12a, the same tendency as in the previous case is observed, i.e., a decrease in Te as the ship's speed increases. However, erratic behaviour in the Te tendency is clearly observed in Figure 12b, except for α = 100° and 110° where a smooth progressive increase is deducted. What is more, for this particular case of Tw, the maximum value of Te is reached with α = 130°, and from this value onwards, a reduction in Td is produced. Specifically, with α = 130° the Te tendency is to be infinite, as can be observed. However, to better illustrate the purposes of the remaining α conditions, the Te is only represented until 300 s.

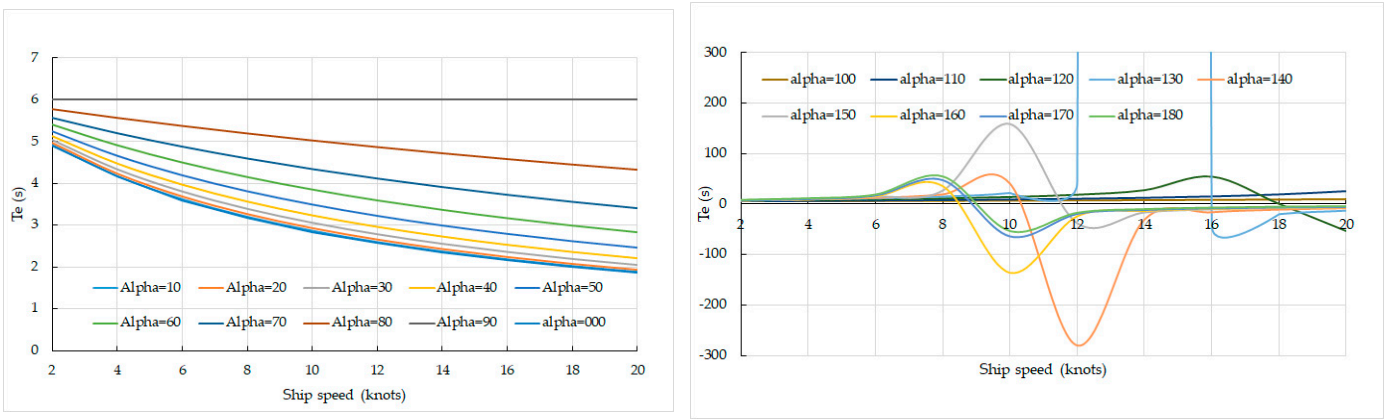

(**a**) (**b**)

Figure 12. The Te for different combinations of ship speeds and α angles for a Tw = 6 s, (**a**) corresponding to α angles between 000° and 90° and (**b**) α angles between 100° and 180°.

In order to analyse the Te behaviour for cases of α > 90°, Figure 13 shows the corresponding graphs for Tw = 3 s (a) and Tw = 10 s (b). It is observed that in the lower Tw, erratic behaviour is produced at lower ship speeds and vice versa. Similar to the previous figure, for Tw = 10 s (b), with α = 160°, a tendency to the infinite is clearly observed, but for clarifying purposes of the remaining α conditions related to the scale, this curve is not completely represented.

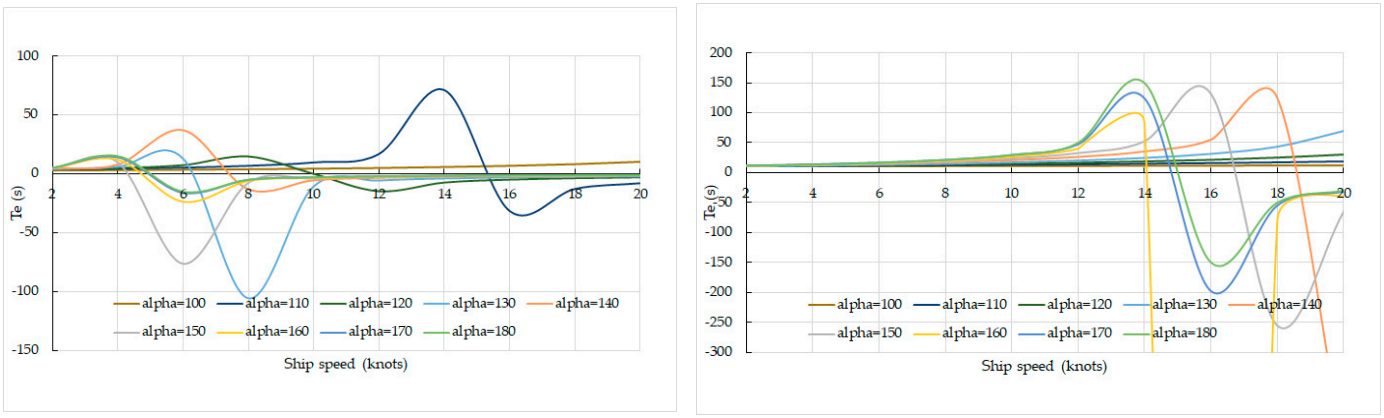

(**a**) (**b**)

Figure 13. The Te for different combinations of velocities and α angles. (**a**) Tw = 3 s and (**b**) Tw = 10 s.

In view of these relevant results, the common practice of reducing the ship's speed and changing the heading in order to receive the waves by the bow is not always the best solution for all cases. What is more, when sailing in bad weather conditions, when the

shipmaster decides to alter the heading and/or the ship's speed in order to improve the seakeeping and ship's behaviour during the rolling motion, he must analyse the response of the ship in the near future. With such a decision, it should be noted that in playing with the relationship between the Vs, Vw, and an α angle, a new Te is reached, and the coupling time is changed to smooth sea conditions arriving earlier or later. This change in the coupling time allows the shipmaster to have sufficient time to modify, for example, the ship's loading conditions, ballasting, deballasting, or transferring weights vertically.

Finally, according to the same procedure followed in the previous sub-sections, for a Te value instead of Tw, Equation (40) changes to:

$$\theta_{MIN} = \theta_M \cdot e^{-\lambda \cdot t} + \frac{\theta_{MW}}{1 - \frac{Td^2}{Te^2}} \quad (45)$$

with Equation (45), once Td and Te are known and the minimum admissible rolling angle (θ_{MIN}) is established, it is possible to calculate this very important new time (t) of coupling.

4. Discussion

As it was shown previously that once a consistent period of time elapses, ships with any loading condition are going to roll according to waves' frequencies, in this section, it is discussed whether a similar behaviour is produced when an idle ship with a certain loading condition is under the influence of different sea state conditions. For that purpose, a loading condition of Td = 12 s, considered representative enough of most merchant fleets in normal ballast or loading conditions, is selected. Without considering a Tw = 12 s, which corresponds to a synchronism phenomenon and whose results would not be representative, the condition for waves far away from Tw with the same values in excess and deficit, i.e., Tw = 6 s, 10 s, 14 s, and 18 s, were studied. Figure 14 shows the roll angles of the mentioned studied case while keeping the roll damping coefficient (0.015) and the maximum initial rolling angle (8.0°). From Figure 10, it can be seen that no coupling of frequencies is produced between different sea state conditions. However, it is worth noting that once the first 200 s elapses, the ship is going to roll with a constant roll angle amplitude and period. Furthermore, it is relevant to note that higher rolling angles are reached with Tw = 14 s than, for instance, with Tw = 18 s, this last case being a worst sea state condition. This result can be related to being in the vicinity of the synchronism phenomenon, which can be studied in more detail in future research works.

Concerning the obtained results of the rolling angles registered to opposites sides, when Td < Tw or Td > Tw, at zero-speed conditions and under the influence of beam waves, it can be concluded that they do not have relevance when a single ship is studied. However, this conclusion can be relevant in ship-to-ship operations (lightering or bunkering, for example), where the loading condition of both ships is changed permanently. The fact that coupling occurs, but that each ship reaches this coupling by rolling to the opposite side of the other ship, can produce damage to the fenders or structures.

Regarding sailing in dynamic conditions, with the ship at a non-zero speed and receiving waves from any direction (α), if a Te is considered, for instance, at double the ship's speed with respect to the wave velocity (Vs/Vw = 2) and an α angle of 0.20 rad, the new Te will be one-third of the Tw. In consequence, the coupling time changes to smooth sea conditions. Therefore, by changing the ship's speed (Vs) and heading (α) with the same ship's loading condition (Td), it is possible to reduce the rolling angle and its consequences such as the coupling time and the maximum angle. Furthermore, according to Equation (41), by changing the ship heading angle or speed, the time to reach the maximum rolling angle will shorten (one-third of the time). For instance, for an encounter period of one-third of the waves' period, the dynamic coupling time will change in this same proportion, and it is reduced by one-third. At the same time, the maximum rolling angle is reduced as well.

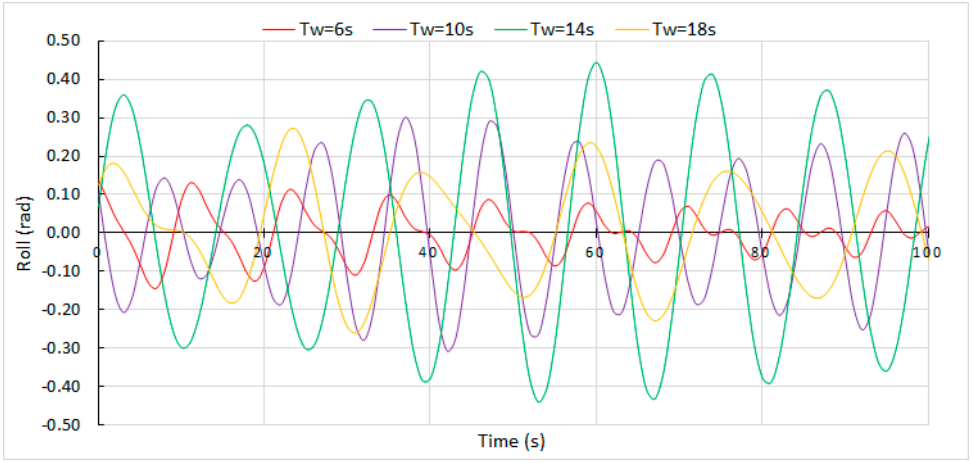

(**a**)

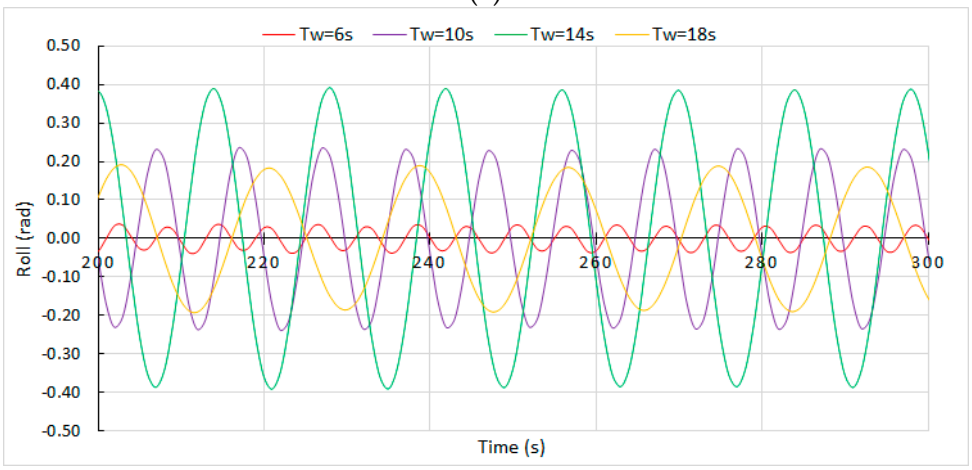

(**b**)

Figure 14. Rolling angles reached with different sea state conditions for Td = 12 s, (**a**) from 0 to 100 s and (**b**) from 200 s to 300 s.

With the aim of providing a practical guide for shipmasters, Figure 15 intends to show and relate in a 3D map the three main variables at play during navigation, i.e., the two navigational parameters to be controlled by ship operators (ship speed and heading angle, α), and Te, a result of the relationship between wave's characteristics and the navigational parameters. For this reason, in the first two cases, a Tw = 18 s (a) and Tw = 21 s (b) are depicted, i.e., very rough sea state conditions. As it can be observed, the maximum Te is registered at the maximum ship speed and with the maximum α angles, i.e., following the seas. This tendency is also observed with Tw = 14 s (c), registering a very high relative peak at the maximum ship speed and α angle. This sea state condition can be considered as the limit of a 3D smooth surface, resulting in the progressive increase in Te with the ship's speed and α angle. This statement can be corroborated after representing the cases for Tw = 10 s (d), Tw = 6 s (e), and Tw = 3 s (f). From them, it is deduced that the maximum Te is not reached at the maximum ship speed and with α angles near the beam. In fact, it is shown that negative values are produced, which means that the possibility of encountering the period has already been exceeded. However, these negative values are very close to the positive values of very high relative values, which means that any minimal changes in ship speed or α angle will imply a very different situation, which has to be considered by shipmasters. It is also important to notice the very high peak value that occurs when Tw = 6 s, in spite of it being a smooth sea state condition.

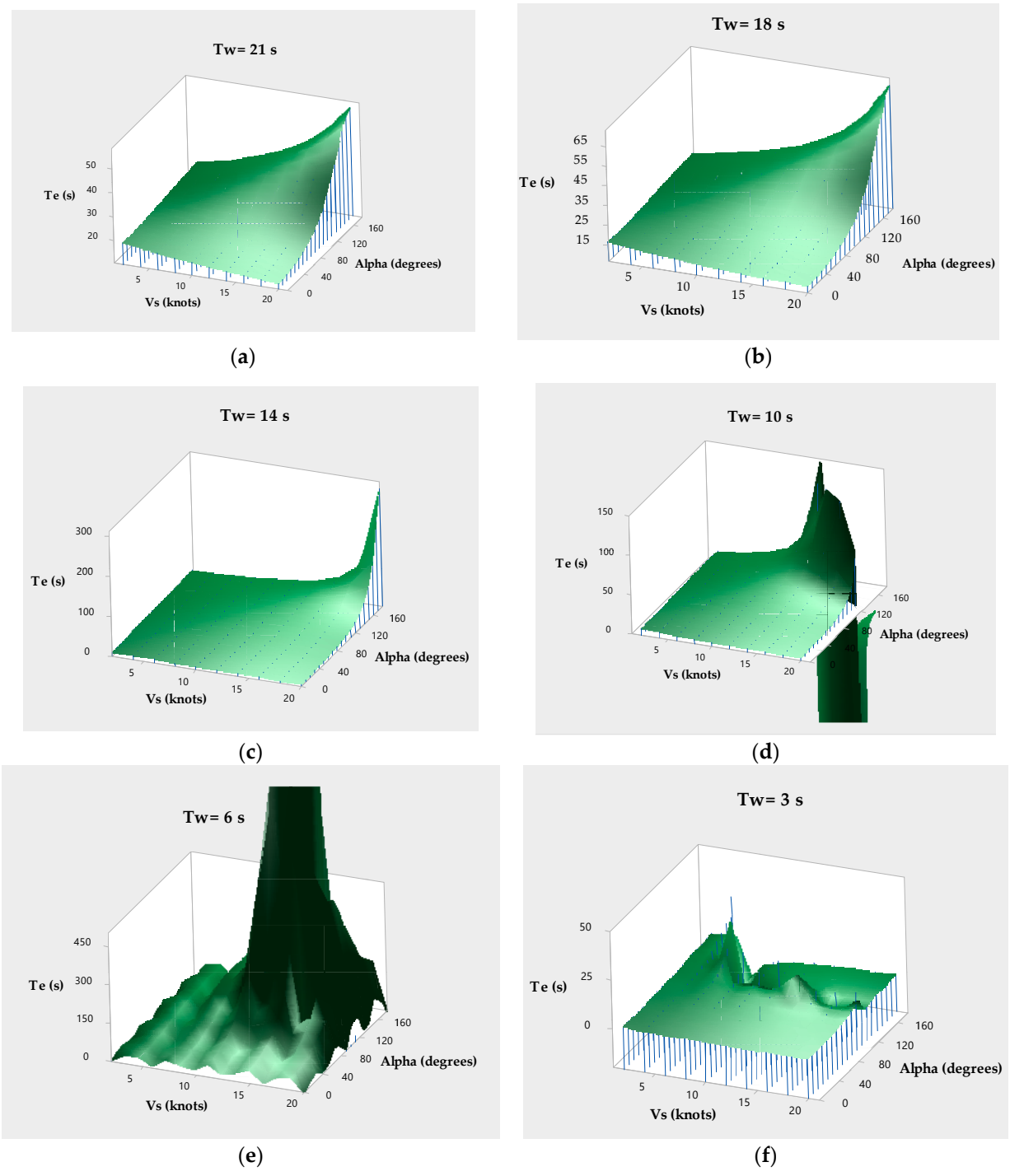

Figure 15. Surface graphs for different sea state conditions. (**a**) Tw = 21 s; (**b**) Tw = 18 s; (**c**) Tw = 14 s; (**d**) Tw = 10 s; (**e**) Tw = 6 s; and (**f**) Tw = 3 s.

Therefore, although initially and from a mathematical point of view, it could be thought that the highest Te values would occur at low ship speeds and with α angles close to the beam, it has been shown that this is not the case. Thus, in our opinion, the use of these original guides can be very useful for shipmasters to avoid dangerous situations on board, related to very large rolling angles before coupling occurs, and even the synchronism phenomenon, which causes the ship to capsize. However, although in some Figure 15d,e there are values out of the axes limit (tending to be infinite), it was represented in this way for the clarifying purposes of the remaining conditions.

Knowing that the synchronism situation is reached when Te and Td are equal, and considering Equation (39) and all sea state conditions (21 types), it was studied which α angles should be avoided for speeds from 2 to 12 knots, at intervals of 2 knots. A polar diagram with the results of combinations that produce synchronism for a Td = 9 s, where 0° and 360° correspond to the forward and 180° the stern, is shown in Figure 16. Each of the concentric circles represents the ship's speed.

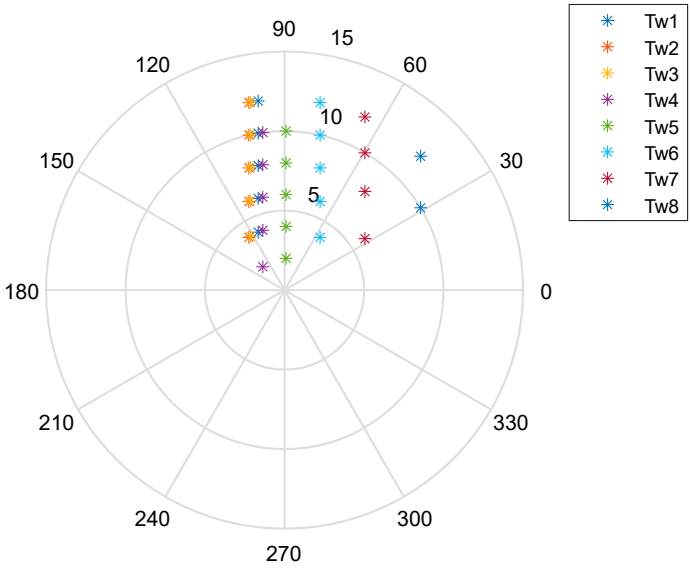

Figure 16. Polar diagram of synchronism representing α angle for different ship speeds.

As it is shown, the only probability of synchronism occurs from 1 s < Tw < 8 s, i.e., for the lowest value of Tw, and within these ranges, a higher probability occurs for even the lowest values. Therefore, contrary to what might be supposed, synchronism does not occur only in the worst sea state conditions, a fact that shipmasters must take into account. Obviously, although the synchronism is only represented at the port side, considering symmetry, the same occurs at the starboard side.

Another relevant result is that the possibilities of synchronism are concentrated for about 30° < α < 110°, i.e., the safest options to avoid it would be to receive the waves from quarter to aft, and more towards the forward.

An important conclusion obtained from Figure 16 is that for a given ship's loading condition (Td) and waves (Tw and Lw), the limit condition of synchronism occurrence is constant and has a linear relationship determined by the ship's speed and α angle. Therefore, if the shipmaster decides to alter the speed (Vs) and the heading (α) at the same time in order to avoid synchronism, he must consider that the result of the product must be substantially different from the limiting value in order to avoid a new dangerous situation.

From Equation (39) it is also possible to know what ship speed must be avoided when the shipmaster prefers not to alter the heading, i.e., when the α is constant. Figure 17 depicts a polar diagram of the obtained results after analysing the 21 sea state conditions. It is shown that potential synchronism situations are produced for 1 s < Tw < 10 s, i.e., for the lowest Tw or similar, without being considered very rough seas. In this case, it is possible to find synchronism in more sea state conditions (Tw = 9 and 10 s) than in the previously mentioned study. Furthermore, the graph shows us that the potential synchronism is concentrated from forward to a little after the beam.

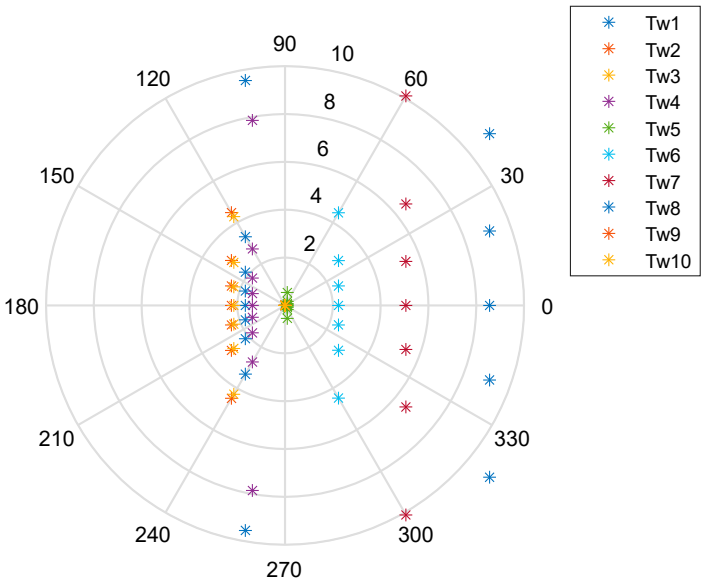

Figure 17. Polar diagram of the synchronism representing ship speeds for different α angles.

Therefore, with the results obtained from polar diagrams, it is deduced that the extreme peaks registered in Figure 15, corresponding to erratic behaviour, are related to moments of synchronism occurring. Furthermore, the results of both approaches are concordant.

The Spanish Commission for Investigation of Maritime Accidents and Incidents (CIAIM) issued a technical report about the accident of the fishing vessel SIN QUERER DOS [35], where four crewmembers died in Galician waters in December 2018. It was concluded that the sudden capsizing and sinking of the vessel was caused by deficient stability, mainly related to a negligent shipment of fishing nets with excessive weight and size. From this report, it was obtained that the ship was sailing with a course of about 160°; with wind from the west at a force 5 (gusts of force 7) on the Beaufort scale; and a swell from the west with wave heights between 4 m and 5 m, corresponding to 8 s < Tw with a median < 9 s. The ship was sailing freely after a fishing campaign, so it could have been sailing with a speed between 7 and 10 knots. According to the data included in the report, the α angle between the ship's heading and the waves' direction was about 110°. Therefore, considering the parameters of the ship's speed and α angle, according to our conclusions expressed in Figure 17, at the moment of the accident the ship could have been involved in a synchronism phenomenon. However, in spite of this, there was no mention included in the report of the ship's behaviour and seakeeping in dynamic situations when sailing between waves.

Therefore, the mathematical models, graphs, and results presented in this paper could be considered by ship operators, by investigating equipment regarding sudden losses of stability (mainly fishing vessels), or by investigating the potential damages due to cargo shifting on board merchant vessels due to an excessive angle of rolling.

With the use of these guides, shipmasters have a useful tool when they decide to change the ship's speed and heading, depending on the available time, to reach a new stable condition. Furthermore, it was deduced that when a shipmaster alters the heading in order to receive the waves forward the beam, the Te tendency to reach the coupling is linear with the ship's speed. However, if after performing the heading alteration the waves are received abaft the beam, the shipmaster must carry out a deep study of the situation. The shipmaster may need to reach the Te quickly or, conversely, he may need to lengthen the time at which the rendezvous is reached in order to alter, for example, any other situations on board such as reinforcing the lashing system or changing the loading conditions.

In consequence, as a guide for shipmasters, it is proposed to improve navigation by selecting adequate values of ship velocity and heading angle in accordance with our previous conclusions. This relation, due to the limitations in reducing the ship's speed

to reasonable and energetic minimum requirements, has a limitation in changes. Despite this, changing the heading angle will help to reach, until the coupling process is finished, an adequate rolling angle and, what is more, change the time to adjust to these new sea conditions.

In this sense, these results can be considered a guide for navigation consideration when experiencing new sea conditions. In particular, to change the Tw to a new Te, one must consider the Td value to make it as far away from this as possible to prevent synchronous situations.

5. Conclusions

In the present research, a ship's behaviour in a rolling motion was analysed and mathematically modelled. Firstly, it was modelled in zero-speed conditions, from a theoretical point of view, when the ship is subjected to a single and external force as a result of its own restoring moment. For some given initial assumptions, and after considering different studied cases, it was found that after the first 300 s, the angle of the rolling motion is practically nil, regardless of the ship's loading condition. Then, it was demonstrated that, contrary to what may be considered, in the long-time domain, the initial mass distribution does not influence the time to recover the upright position. A very simple mathematical relationship that shows the time needed to reach the maximum rolling angle was found, the results of which were corroborated with the corresponding angular velocities.

Afterwards, once the full spectrum of sea state conditions was modelled, the mathematical models of the ship's rolling motion under the influence of beam waves with resistance, in a long-time domain and at zero-speed conditions, were obtained. In this case, relevant results were found. After the first 150–200 s and onwards, it was shown that the coupling of roll frequencies with waves' periods was periodically repeated with the same amplitude, regardless of the ship's loading condition. What is more, once this period of time elapsed, the ship rolls according to the waves' frequency, i.e., the ship's loading conditions are not relevant. This is an aspect essential to the ship's overall safety and its behaviour at sea. For instance, the cargo lashing design should consider the transversal accelerations sustained by the ship during the sea route, not the roll angle amplitude. For this reason, the results here obtained can be considered useful for ship operators given that it allows them to know, well in advance, from what moment there will be no sudden increases in acceleration which cause the lashing to break. Furthermore, in the case of passenger ships, it can be known ahead of time how to reach a stable condition as smoothly as possible for the passengers' comfort. This condition implies the worst stability (i.e., a higher Td), but it is remarkable to know that, after a certain period of time, the ship will roll according to the waves' frequencies. However, as it was also graphically shown, in the first moments under the influence of waves, the behaviour of each ship depends on the relationships between Td and Tw. Lastly, a mathematical model which allows for the calculation of the time to reach the coupling frequencies for a given rolling angle was obtained.

The results of these two first studies are valid considering certain assumptions such as the ship at zero speed under the influence of beam waves, and linear factors during the rolling motion.

Finally, the ship's rolling motion while sailing in waves coming from any constant direction and the ship sailing at non-zero speed was studied. In these universal conditions, the encounter period (Te) replaces the wave's period (Tw) as being the most influential in the ship's behaviour. For that reason, as the shipmaster has influence in the mentioned Te to modify navigational parameters such as the heading and ship's speed, a guide for shipmasters in the form of a 3D map and polar diagrams is proposed to improve the safety of navigation by enabling the selection of adequate values for the ship's speed and heading angle, depending on the sea conditions found. In particular, changing the heading angle and/or ship's speed will help to reach, until the coupling process is finished, an adequate rolling angle and, moreover, change the time to adjust to these relatively new sea conditions.

It even indicates the ship speeds and α angles to avoid in order to stay as far away as possible from synchronism conditions.

Future studies and research can be guided to validate the present theoretical results in towing tank tests with scale ships or in virtual simulations using computer programmes. These simulated research works, in addition to validating the presented results, can be used as a training tool for ship operators to obtain more realistic guidelines on how they should act in different sea state conditions, anticipating as quickly as possible dangerous situations on board related to a rolling motion.

Author Contributions: Conceptualisation, J.M.P.-C. and J.A.O.; methodology, J.M.P.-C., J.A.O., F.J.P.-C. and V.D.-G.; validation, J.M.P.-C., J.A.O., F.J.P.-C. and V.D.-G.; formal analysis, J.M.P.-C., J.A.O., F.J.P.-C. and V.D.-G.; investigation, J.M.P.-C., J.A.O., F.J.P.-C. and V.D.-G.; data curation, J.M.P.-C., J.A.O., F.J.P.-C. and V.D.-G.; writing—original draft preparation, J.M.P.-C. and J.A.O.; writing—review and editing, J.M.P.-C., J.A.O., F.J.P.-C. and V.D.-G. All authors have read and agreed to the published version of the manuscript.

Funding: This work was funded by the University of A Coruña and the University of Cádiz, grant number 63.10.G4.92.23.

Institutional Review Board Statement: Not applicable.

Informed Consent Statement: Not applicable.

Data Availability Statement: Not applicable.

Conflicts of Interest: The authors declare no conflict of interest.

Appendix A

Table A1. Symbols and their definitions.

Symbol	Definition
Ma	Ship's righting moment
Ig	Inertia moment of the ship's mass
D	Ship's displacement
GM	Transverse metacentric height
Td	Ship's natural rolling period
A_R	Damping coefficient
g	Gravity acceleration
k	Turning radius of the ship's mass
Lw	Wavelength
Tw	Wave period
Vw	Wave translation velocity
Hw	Wave height
Aw	Wave amplitude
Vs	Ship's speed
Te	Encounter period
α	Angle formed between the heading and wave influence direction
θ_{MW}	Maximum wave slope
θ_W	Wave slope
θ	Rolling angle
θ_M	Maximum initial rolling angle
ω_W	Wave frequency
ω_1	Damped ship's natural roll frequency
λ	Rolling damping factor
2λ	Relation between AR and Ig
ω	Ship's natural roll frequency
θ'_{RM}	Angular velocity of the initial restoring moment
θ'_W	Angular velocity of the dynamic condition of the waves

References

1. Lu, J.; Gu, M.; Boulougouris, E. Further Study on One of the Numerical Methods for Pure Loss of Stability in Stern Quartering Waves. *J. Mar. Sci. Eng.* **2023**, *11*, 394. [CrossRef]
2. Petacco, N.; Gualeni, P. IMO second generation intact stability criteria: General overview and focus on operational measures. *J. Mar. Sci. Eng.* **2020**, *8*, 494. [CrossRef]
3. Marlantes, K.E.; Kim, S.; Hurt, L.A. Implementation of the IMO Second Generation Intact Stability Guidelines. *J. Mar. Sci. Eng.* **2022**, *10*, 41. [CrossRef]
4. Acanfora, M.; Balsamo, F. The smart detection of ship severe roll motions and decision-making for evasive actions. *J. Mar. Sci. Eng.* **2020**, *8*, 415. [CrossRef]
5. Semenova, V.; Rozhdestvensky, K.; Albaev, D.; Htet, Z.M. Study of the Influence of Nonlinear Moments upon Intensity of Parametric Roll. *J. Mar. Sci. Eng.* **2022**, *10*, 1164. [CrossRef]
6. Khan, N.A.; Sulaiman, M.; Tavera Romero, C.A.; Laouini, G.; Alshammari, F.S. Study of Rolling Motion of Ships in Random Beam Seas with Nonlinear Restoring Moment and Damping Effects Using Neuroevolutionary Technique. *Materials* **2022**, *15*, 674. [CrossRef]
7. Im, N.; Lee, S. Effects of Forward Speed and Wave Height on the Seakeeping Performance of a Small Fishing Vessel. *J. Mar. Sci. Eng.* **2022**, *10*, 1936. [CrossRef]
8. Geng, X.; Li, Y.; Sun, Q. A Novel Short-Term Ship Motion Prediction Algorithm Based on EMD and Adaptive PSO–LSTM with the Sliding Window Approach. *J. Mar. Sci. Eng.* **2023**, *11*, 466. [CrossRef]
9. Xie, X.; Li, M.; Du, X. Nonlinear dynamics of marine rotor-bearing system coupled with vibration isolation structure subject to ship rolling motion. *Appl. Math. Model.* **2022**, *103*, 344–359. [CrossRef]
10. Long, Z.-J.; Lee, S.-K.; Jeong, J.-H.; Lee, S.-J. Study for the safety of ships' nonlinear rolling motion in beam seas. *J. Navig. Port Res.* **2009**, *33*, 629–634. [CrossRef]
11. Sun, H.-B.; Yang, S.-Q.; Xu, Y.-F.; Xiao, J.-F. Prediction of the Pitch and Heave Motions in Regular Waves of the DTMB 5415 Ship Using CFD and MMG. *J. Mar. Sci. Eng.* **2022**, *10*, 1358. [CrossRef]
12. Lee, S.; You, J.-M.; Lee, H.-H.; Lim, T.; Take Park, S.; Seo, J.; Hyung Rhee, S.; Rhee, K.P. Experimental Study on the Six Degree-of-Feedom Motions of a Damaged Ship Floating in Regular Waves. *IEE J. Ocean. Eng.* **2016**, *41*, 40–49. [CrossRef]
13. Liu, Y.; Hu, A.; Han, F.; Lu, Y. Stability analysis of nonlinear ship-roll dynamics under wind and wave. *Chaos Solitons Fractals* **2015**, *76*, 32–39. [CrossRef]
14. Li, Y.; Wei, Z.; Kapitaniak, T.; Zhang, W. Stochastic bifurcation and chaos analysis for a class of ships rolling motion under non-smooth perturbation and random excitation. *Ocean Eng.* **2022**, *266*, 112859. [CrossRef]
15. Mai, T.L.; Vo, A.K.; Yoon, H.K.; Park, D.K. Assessment of the Roll Derivatives of Different Surface Ships Based on Numerical Pure Roll Simulation. *J. Mar. Sci. Eng.* **2022**, *10*, 1702. [CrossRef]
16. Buca, P.; Senjanovic, I. Nonlinear ship rolling and capsizing. *Brodogradnja* **2006**, *57*, 321–331.
17. Cai, G.Q.; Zhu, W.Q. Generation of two correlated stationary Gaussian processes and application to ship rolling motion. *Probabilistic Eng. Mech.* **2019**, *57*, 26–31. [CrossRef]
18. Liu, L.; Feng, D.; Wang, X.; Zhang, Z.; Yu, J.; Chen, M. Study on extreme roll event with capsizing induced by pure loss of stability for the free-running ONR Tumblehome. *Ocean Eng.* **2022**, *257*, 111656. [CrossRef]
19. CSS Code. *Safe Practice for Cargo Stowage and Securing*; International Maritime Organization (IMO): London, UK, 2021.
20. Yao, J.; Cheng, X.; Song, X.; Zhan, C.; Liu, Z. RANS Computation of the Mean Forces and Moments, and Wave-Induced Six Degrees of Freedom Motions for a Ship Moving Obliquely in Regular Head and Beam Waves. *J. Mar. Sci. Eng.* **2021**, *9*, 1176. [CrossRef]
21. Fan, X.; Hu, Z.; Zheng, X. Research on Influence of Tank Sloshing on Ship Motion Response under DifferentWavelengths. *Appl. Sci.* **2022**, *12*, 8647. [CrossRef]
22. Hu, L.; Wu, H.; Yuan, Z.; Li, W.; Wang, X. Roll motion response analysis of damaged ships in beam waves. *Ocean Eng.* **2021**, *227*, 108558. [CrossRef]
23. Gao, Q.; Song, L.; Yao, J. RANS Prediction of Wave-Induced Ship Motions, and Steady Wave Forces and Moments in Regular Waves. *J. Mar. Sci. Eng.* **2021**, *9*, 1459. [CrossRef]
24. Mahfouz, A.B. Identification of the nonlinear ship rolling motion equation using the measured response at sea. *Ocean Eng.* **2004**, *31*, 2139–2156. [CrossRef]
25. Guo, B.J.; Steen, S.; Deng, G.B. Seakeeping prediction of KVLCC2 in head waves with RANS. *Appl. Ocean Res.* **2012**, *35*, 56–67. [CrossRef]
26. He, T.; Feng, D.; Liu, L.; Wang, X.; Jiang, H. CFD Simulation and Experimental Study on Coupled Motion Response of Ship with Tank in BeamWaves. *J. Mar. Sci. Eng.* **2022**, *10*, 113. [CrossRef]
27. Pérez-Canosa, J.M.; Orosa, J.A.; Fraguela, F.; López-Varela, P. Proposal of Optimal Operation in Ship Rolling Motion Considering Sea State Conditions. *J. Mar. Sci. Eng.* **2022**, *10*, 669. [CrossRef]
28. Pérez-Canosa, J.M.; Orosa, J.A.; Galdo, M.I.L.; Barros, J.J.C. A New Theoretical Dynamic Analysis of Ship Rolling Motion Considering Navigational Parameters, Loading Conditions and Sea State Conditions. *J. Mar. Sci. Eng.* **2022**, *10*, 1646. [CrossRef]
29. Medina, M. *The Sea and the Weather. Nautical Meteorology*, 3rd ed.; Juventud: Barcelona, Spain, 2007.
30. *International Code on Intact Stability, 2008*; International Maritime Organization (IMO): London, UK, 2020.

31. Bonilla de la Corte, A. *Ship's Theory*, 4th ed.; Librería San José: Vigo, Spain, 1994.
32. DNV. Rules for Classification of Ships. Part 3. Chapter 1. Hull Structural Design—Ships with Length 100 Metres and Above. 2016. Available online: http://rules.dnvgl.com/docs/pdf/dnv/rulesship/2016-01/ts301 (accessed on 30 August 2022).
33. Woo, D.; Choe, H.; Im, N.-K. Analysis of the Relationship between GM and IMO Intact Stability Parameters to Propose Simple Evaluation Methodology. *J. Mar. Sci. Eng.* **2021**, *9*, 735. [CrossRef]
34. Valle-Cabezas, J. Estudio teórico experimental de las no linealidades del amortiguamiento en el movimiento de balance de buques. Ph.D. Thesis, Universidad Politécnica de Madrid, Madrid, Spain, 1998.
35. Ministerio de Transportes, Movilidad y Agenda Urbana. Gobierno de España. Informe CIAIM-22/2020. Vuelco y Hundimiento del Buque de pesca SIN QUERER DOS a 4,5 millas al sur de Finisterre, el día 19 de Diciembre de 2018, con Resultado de tres Tripulantes Fallecidos y un Desaparecido. 2020. Available online: https://www.mitma.gob.es/recursos_mfom/comodin/recursos/ic_22-2020_sin_querer_dos_web.pdf (accessed on 10 March 2023).